Dendrite fragmentation in alloy solidification due to sidearm pinch-off

Supplementary information

H. Neumann-Heyme* and K. Eckert
Institute for Fluid Dynamics, Technische Universität Dresden, 01062 Dresden, Germany

C. Beckermann
Department of Mechanical and Industrial Engineering, The University of Iowa, Iowa City, IA 52242, USA

1. Phase-field model

The simulations in the present work are based on the quantitative phase-field model for alloy solidification that is described in [1]. In the case of vanishing interface kinetics and interface anisotropy, the phase field equations read as follows

$$[1-(1-k)\theta]\,\partial_t\Phi = \nabla^2\Phi+\Phi-\Phi^3-\lambda\left(1-\Phi^2\right)^2(U-\theta) \quad \text{(A.1)}$$

$$[1+k-(1-k)\Phi]\,\partial_t U = \nabla\cdot\left[a_2\lambda(1-\Phi)\nabla U+\vec{j}_{\rm at}\right] + [1+(1-k)U]\,\partial_t\Phi, \quad \text{(A.2)}$$

where k, Φ, λ and $\vec{j}_{\rm at}$ are the partition coefficient, phase-field variable, coupling coefficient, and corrective anti-trapping current, and $a_1 = 0.8839$, $a_2 = 0.6267$ are constants. The scaled supersaturation and temperature are given, respectively, by

$$U = \frac{1}{1-k}\left[\frac{2c/c_l^0}{1-\Phi+k(1+\Phi)}-1\right] \quad \text{(A.3)}$$

and

$$\theta = \frac{T_0-T}{|m|c_l^0(1-k)}, \quad \text{(A.4)}$$

where T, c, m are temperature, solute concentration and liquidus slope, and c_l^0 is the equilibrium liquid concentration at the initial temperature $T = T_0$. Length and time are non-dimensionalized by the diffuse interface width $W_0 = d_0\lambda/a_1$ and kinetic coefficient $\tau_0 = a_2 d_0^2\lambda^3/a_1^2 D$, respectively, where D and d_0 are solute diffusivity in the melt and chemical capillary length.

According to the thin interface asymptotic analysis of Ref. [1], convergence of the phase-field model towards the sharp interface model given by Eqs. (1-3) in the article is achieved by choosing a diffuse interface width that is small enough that the solution becomes independent of the interface width. This interface width must be scaled by the characteristic length scale of the problem, which in the present study is given by the initial sidearm radius, R. A converged solution is thus achieved for a certain small but finite value of the ratio W_0/R. As described in the article, the present model is simplified by assuming that $d_0/R \to 0$. In view of the definition of W_0 given above, this limit would imply that for a finite ratio W_0/R, the coupling constant λ would tend to infinity. A λ that tends to infinity would, however, render the numerical solution of Eqs. (A.1,A.2) ill-conditioned. In order to avoid this problem, Eqs. (A.1,A.2) are rewritten in terms of $\bar{U} = (U-\theta)/\epsilon$ where $\epsilon = 1/a_2\lambda$, which yields

$$[1-(1-k)\theta]\,\partial_t\Phi = \nabla^2\Phi+\Phi-\Phi^3-\frac{\bar{U}}{a_2}\left(1-\Phi^2\right)^2 \quad \text{(A.5)}$$

$$[1+k-(1-k)\Phi]\left(\epsilon\partial_t\bar{U}+\dot{\theta}\right) = \nabla\cdot\left[(1-\Phi)\nabla\bar{U}+\vec{j}_{\rm at}\right] + \left[1+(1-k)\left(\epsilon\bar{U}+\theta\right)\right]\partial_t\Phi, \quad \text{(A.6)}$$

where $\dot{\theta}$ is the scaled cooling rate in terms of the dimensionless time used in the phase-field model. In the limit $\epsilon \to 0$, Eq. (A.6) then reduces to

$$[1+k-(1-k)\Phi]\,\dot{\theta} = \nabla\cdot\left[(1-\Phi)\nabla\bar{U}\right] + [1+(1-k)\theta]\,\partial_t\Phi. \quad \text{(A.7)}$$

Since $d_0/R \to 0$ corresponds to the limit of low interface velocities, the anti-trapping current $\vec{j}_{\rm at}$ in Eq. (A.6) is omitted in Eq. (A.7). According to our axisymmetric model all equations are solved in cylindrical coordinates.

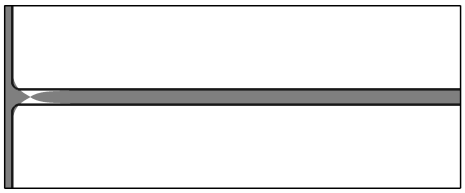

FIG. 1. Projected geometry of the isothermal, long sidearm case ($\Lambda_2/R = 12$, $\Lambda_1/R = 60$); thick line: initial state at $t = 0$; solid grey: pinch-off at $t = 0.53R^3/Dd_0$.

* hieram.neumann-heyme@tu-dresden.de

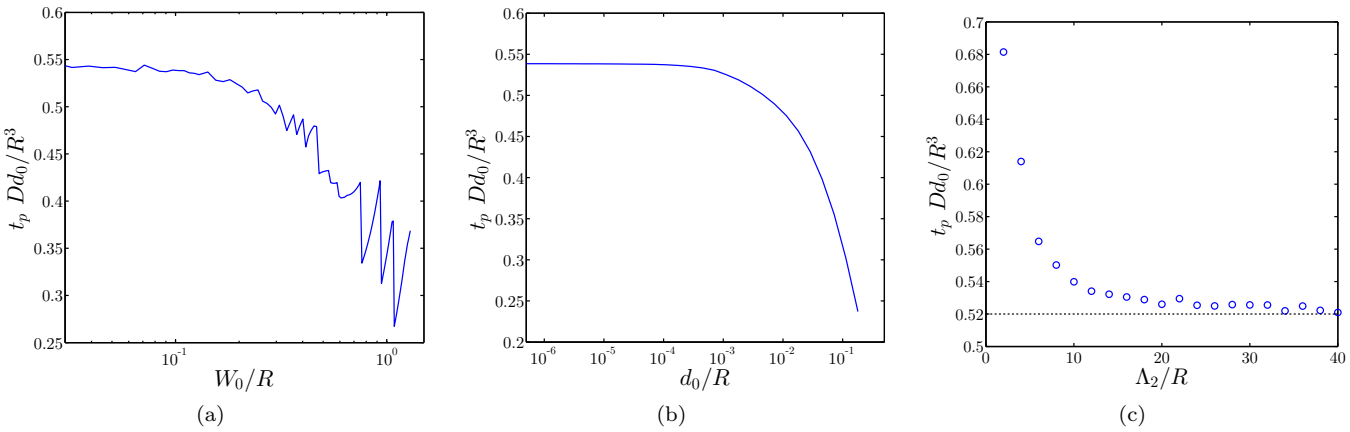

FIG. 2. Results for the isothermal long sidearm case. (a) Dimensionless pinch-off time vs. interface width. (b) Dimensionless pinch-off time vs. capillary length. (c) Dimensionless pinch-off time vs. spacing Λ_2.

The computational domain is discretised by triangular elements. The local element size is controlled by the magnitude of the solute concentration gradient. Further, it is required, that in the maximum refined region at the interface the longest edge of an element is less than $0.7W_0$. Since the mesh refinement works by repeated bisectioning of a coarse macro-mesh, the element size can only have discrete values of $\Lambda_2/2^{n/2}$, where $n \in \mathbb{N}$. In cases, where Λ_2/R and W_0/R are varied continuously, the discrete nature of the minimum element size can cause small scatter of the results, e.g. Fig. 2a and 2c.

Time steps are adjusted according to the normal interface velocity V_n as $\Delta t = 0.15/\max(V_n)$. This method prescribes the maximum distance the interface can advance in a given time step. When considering the long sidearm limit, the domain length Λ_1 is chosen as $\Lambda_1 = 5\Lambda_2$, which was verified to be large enough for the solution to be independent of Λ_1.

In the following, a few general aspects regarding validity and convergence of the model are discussed. The calculations are for the long sidearm case under isothermal conditions, with $\Lambda_2/R = 12$ and $\Lambda_1/R = 60$, as shown in Fig. 1.

2. Convergence

Convergence of the presented model with respect to the interface width of the phase-field is analyzed in Fig. 2a by plotting the scaled pinch-off time $t_p Dd_0/R^3$ as a function of W_0/R. Note that this physically motivated scaling, used throughout the article, is different from that for the phase-field model, Eqs. (A.1-A.7). An acceptable accuracy of the results is archived for $W_0/R = 0.1$. This value is used in most calculations of the present study. This rather fast convergence is due to the fact that, even though close to pinch-off the essential length κ_φ^{-1} becomes arbitrary small, the duration of this final collapse is small compared to the time of the entire process. For the study of the critical finger length for the transition between retraction and pinch-off, $l_{r\text{-}p}$, a somehow lower value of $W_0/R = 0.04$ was necessary, since the collapsing tip radius of the arm, seen in the inset of Fig. 4a of the article, has to be resolved, too. The scatter of t_p at larger W_0/R is an indication of the increasing mesh size dependence as discussed earlier.

3. Validity of the quasistationary aproximation of the diffusion field

To study the effect of d_0/R, the pinch-off time was calculated based on Eqs. (A.5,A.6). Figure 2b demonstrates, that the pinch-off time becomes independent of d_0/R for $d_0/R \lesssim 10^{-4}$. This is the essential prerequisite for the validity of Eqs. (5-7) in the article and Eq. (A.7).

4. Lower limit of the pinch-off duration

Another value stated in the article is the large spacing limit of t_p for the isothermal, long arm case. Figure 2c provides the full dependence on the spacing Λ_2. Apart from a moderate increase of $t_p Dd_0/R^3$ towards small Λ_2 due to geometrical restrictions, an asymptotic value of 0.52 is approached soon. This value provides the approximate lower limit for the pinch-off time of a sidebranch subject to solidification.

[1] B. Echebarria, R. Folch, A. Karma, and M. Plapp, Phys. Rev. E **70**, 061604 (2004).